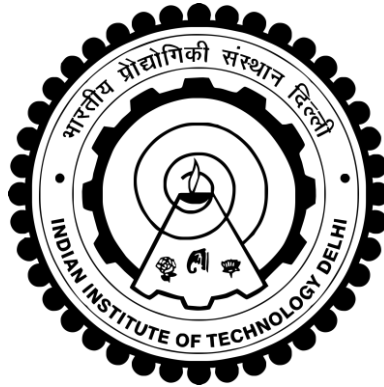


ROLE OF KINETIC ALFVÉN WAVES IN TURBULENCE AND RECONNECTION

RAJESH KUMAR RAI



**CENTRE FOR ENERGY STUDIES
INDIAN INSTITUTE OF TECHNOLOGY DELHI
MAY 2018**

©Indian Institute of Technology Delhi (IITD), New Delhi, 2018

ROLE OF KINETIC ALFVÉN WAVES IN TURBULENCE AND RECONNECTION

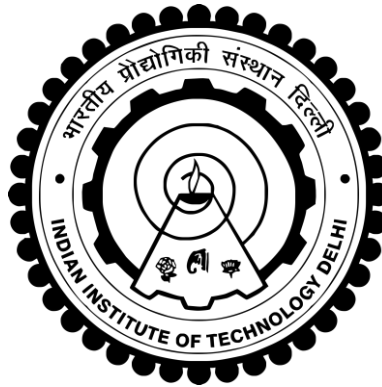
by

RAJESH KUMAR RAI

Centre for Energy Studies

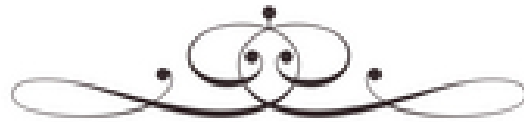
Submitted

*in fulfilment of the requirements of the degree of Doctor of Philosophy
to the*

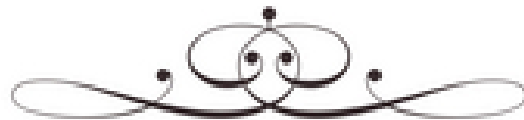


Indian Institute of Technology Delhi

May-2017



Dedicated to
My Supervisor, Parents,
My Wife and son Advik



CERTIFICATE

This is to certify that the thesis entitled “**Role of kinetic Alfvén Waves in Turbulence and Reconnection**” being submitted by **Mr. Rajesh Kumar Rai** to the Indian Institute of Technology Delhi for the award of the Degree of *Doctor of Philosophy*, is a record of bona fide research work carried out by him under my supervision.

The thesis has reached the standards fulfilling the requirements of the regulations relating to the degree. The results contained in this thesis have not been submitted in part or full to any other university or institute for the award of any degree or diploma.

Date:

Place

Dr. R. Uma

Associate Professor

Centre for Energy Studies

Indian Institute of Technology Delhi

New Delhi-110016

Dr. R. P. Sharma

Professor

Centre for Energy Studies

Indian Institute of Technology Delhi

New Delhi-110016

ACKNOWLEDGEMENTS

*I take this opportunity to express deep sense of appreciation towards all those people who have contributed to make this work possible through their help and support along the way. My deepest gratitude and indebtedness goes to my thesis supervisor **Dr. R. Uma** and Co-supervisor **Prof. R. P. Sharma** for giving me the possibility to do this interesting research work and for their trustworthy advices and support through all the phases of the Ph.D. I am indebted to my Co-supervisor for his some remarkable qualities, such as their depth of perception and lucid presentation, perhaps the best I have come across so far, will always continue to inspire me. The experience of working with him, I strongly believe, will have far-reaching influence in my future life.*

I am thankful to all my group members, Alok ji, Nidhi Gaur, Nitin Yadav, Swati Sharma, Ravinder, Prachi and Neha for their cooperation, and support during my research work. With immense pleasure I express my sincere gratitude and feelings towards my parents, my wife, my son and other family members for their patience, and understanding during my research work. I owe it deeply to them for their encouragement and support, which gave me courage and confidence to materialize this work.

Rajesh Kumar Rai

ABSTRACT

Plasma turbulence and magnetic reconnection is an important phenomenon that is present in various space and astrophysical plasmas, for example the solar wind, magnetosphere etc. The present thesis deals with the nonlinear interaction of kinetic Alfvén waves (KAWs) and weak whistler waves taking ponderomotive nonlinearity into account. This thesis also presents the nonlinear evolution of KAWs in the presence of magnetic islands and Harris sheets. The author has studied the coherent structures formation, turbulence, power spectra, magnetic reconnection and particle heating applicable to various solar and magnetospheric plasmas. Numerical simulations of nonlinear KAW dynamics when nonlinearity arises due to ponderomotive effects have been performed. The simulations were performed taking different initial conditions of the pump KAWs *i.e.* longitudinal periodic perturbations, hollow Gaussian, x-o points, transverse periodic perturbation etc. In the second and third chapters of the proposed thesis, the author has studied the nonlinear interaction of KAWs with quasi-transverse and quasi-longitudinal weak whistler waves respectively. In this work, KAWs are pump waves which produce a density modification in the background density through ponderomotive nonlinearity. Whistler waves, propagating in this perturbed medium gets either trapped or localized. It has also been found that the KAWs break up into filamentary structures having high intensity magnetic field. It shows chaotic behavior at the large transverse wavenumber modes and power spectra are consistent with observed Kolmogorov $k^{-5/3}$ scaling. The author has also developed a simplified model in a paraxial regime to understand the

basic physics behind the formation of these localized structures. In the fourth chapter, the author has investigated the role of KAW in the formation of coherent structures/current sheets when it is propagating in the pre-existing fully developed chain of magnetic islands. Due to pre-existing chain of magnetic islands, KAW splits into coherent structures and the scale size of these structures along transverse directions (with respect to background magnetic field) comes out to be order of ion gyro radius. In the fifth chapter, nonlinearity of KAWs is taken into account and it is found that field localization is more intense when the density perturbation due to nonlinearity and field perturbation due to background islands are taken into account simultaneously in comparison to the perturbation created by both the sources separately. The author has also derived the dynamical equation of KAW propagating through Harris sheet having density modification due to nonlinearity and field modification due to the presence of Harris sheet. Due to the presence of background density and field perturbations, Harris sheet gets perturbed and propagating nonlinear KAW shows localization and coherent structures are formed. Based upon these coherent structures analysis, power spectrum has also been evaluated and found the scaling after first breakpoint to be consistent with the observation by Chaston *et al.* [2009]. In the last chapter, It has been studied the importance of electron dynamics in collisionless magnetic reconnection and found that the electrons have a crucial role in forming the structure at the electron inertial length scale and determine the reconnection electric field in magnetic reconnection. Numerical simulation shows that how magnetic island are more chaotic when axial field (electron dynamics) is taken into account.

सार

प्लाज्मा टर्बुलेन्स और चुंबकीय पुनः कनेक्शन एक महत्वपूर्ण घटना है जो विभिन्न अंतरिक्ष और खगोलीय प्लास्मा में मौजूद है, उदाहरण के लिए सौर हवा, चुंबकमंडल इत्यादि। वर्तमान थीसिस गतिशील अल्फवेन तरंगों (केएडब्ल्यू) की अरेखीय बातचीत और कमजोर विह्वल तरंगों को ध्यान में रखते हुए पॉडेरोमोटिव अरेखीय ध्यान रखा गया है। यह थीसिस चुंबकीय द्वीपों और हैरिस शीट्स की उपस्थिति में केएडब्ल्यू के गैर-लाइनर विकास को भी प्रस्तुत करता है। लेखक ने विभिन्न सौर और चुंबकमंडल प्लास्मा के लिए लागू सुसंगत संरचनाओं गठन, टर्बुलेन्स, पावर स्पेक्ट्रा, चुंबकीय पुनः कनेक्शन और कण हीटिंग का अध्ययन किया है। सिमुलेशन पंप केएडब्ल्यू यानी अनुदैर्घ्य आवधिक परेशानियों, खोखले गाऊशियन, एक्स-ओ पॉइंट्स, ट्रांसवर्स आवधिक परेशानी इत्यादि की विभिन्न प्रारंभिक स्थितियों को लेते हुए किया गया है। प्रस्तावित थीसिस के दूसरे और तीसरे अध्यायों में, लेखक ने क्रमशः अर्ध-अनुप्रस्थ और अर्ध-अनुदैर्घ्य कमजोर विह्वल तरंगों के साथ केएडब्ल्यू के गैर-लाइनर बातचीत का अध्ययन किया है। इस काम में, केएडब्ल्यू पंप तरंगों हैं जो पृष्ठभूमि घनत्व में घनत्व संशोधन को पॉडेरोमोटिव अरेखीय के माध्यम से उत्पन्न करते हैं। विह्वल लहरें, इस परेशान माध्यम में प्रचारित या तो ट्रेप या स्थानीयकृत हो जाती हैं। यह भी पाया गया है कि केएडब्ल्यू उच्च तीव्रता चुंबकीय क्षेत्र वाले

फिलामेंटरी संरचनाओं में टूट जाते हैं। यह बड़े ट्रांसवर्स वेवनंबर मोड में कयोटिक व्यवहार दिखाता है और पावर स्पेक्ट्रा कोल्मोगोरोव स्केलिंग के साथ संगत होते हैं। लेखक ने इन स्थानीय संरचनाओं के गठन के पीछे बुनियादी भौतिकी को समझने के लिए एक पैराएक्सियल शासन में एक सरलीकृत मॉडल भी विकसित किया है। चौथे अध्याय में, लेखक ने सुसंगत संरचनाओं / करंट शीट के गठन में केएडब्ल्यू की भूमिका की जांच की है जब यह चुंबकीय द्वीपों की पूर्व-मौजूदा विकसित श्रृंखला में प्रचार कर रहा है। चुंबकीय द्वीपों की पूर्व-विद्यमान श्रृंखला के कारण, केएडब्ल्यू सुसंगत संरचनाओं में विभाजित होता है और इन संरचनाओं के पैमाने के आकार को ट्रांसवर्स दिशाओं (पृष्ठभूमि चुंबकीय क्षेत्र के संबंध में) के साथ आयन जीरो त्रिज्या के क्रम में आता है। पांचवें अध्याय में, केएडब्ल्यू की गैर-रेखाचित्रता को ध्यान में रखा जाता है और यह पाया जाता है कि क्षेत्रीयकरण अधिक तीव्र होता है जब घनत्व में टर्बुलेन्स अरेखीय के कारण होती है और पृष्ठभूमि द्वीपों के कारण क्षेत्र में परेशानी को दोनों के द्वारा बनाए गए परेशानी की तुलना में एक साथ खाते में लिया जाता है। स्रोत अलग से। लेखक ने हैरिस शीट की उपस्थिति के कारण अरैखिकता और क्षेत्र संशोधन के कारण हैरिस शीट के माध्यम से घनत्व संशोधन के माध्यम से प्रचारित केएडब्ल्यू के गतिशील समीकरण को भी प्राप्त किया है। पृष्ठभूमि घनत्व और क्षेत्र में टर्बुलेन्स की उपस्थिति के कारण, हैरिस शीट परेशान हो जाती है और नॉनलाइनर केएडब्ल्यू का प्रचार स्थानीयकरण और सुसंगत संरचनाओं का निर्माण होता है। इन सुसंगत संरचनाओं के विश्लेषण

के आधार पर, पावर स्पेक्ट्रम का भी मूल्यांकन किया गया है और चैस्टन एट अल द्वारा अवलोकन के साथ पहले ब्रेकपॉइंट के बाद स्केलिंग पाया गया है। पिछले अध्याय में, यह टकराव रहित चुंबकीय पुनः कनेक्शन में इलेक्ट्रॉन गतिशीलता के महत्व का अध्ययन किया गया है और पाया गया है कि इलेक्ट्रॉनों की निष्क्रियता के पैमाने पर संरचना बनाने में इलेक्ट्रॉनों की महत्वपूर्ण भूमिका है और चुंबकीय पुनः कनेक्शन में पुनः कनेक्शन विद्युत क्षेत्र निर्धारित करना है। संख्यात्मक अनुकरण से पता चलता है कि चुंबकीय द्वीप अधिक अराजक होता है जब अक्षीय क्षेत्र (इलेक्ट्रॉन गतिशीलता) को ध्यान में रखा जाता है।

CONTENTS

Certificate	i
Acknowledgements	ii
Abstract	iii-iv
List of figures	ix-xii
Chapters	
1. Introduction	1-23
1.1 Background	1
1.2 Plasma models	3
1.2.1 MHD model	3
1.2.2 Two-Fluid Model	7
1.2.3 Kinetic model	9
1.3 Space plasmas	10
1.3.1 The sun	10
1.3.2 Solar Corona	11
1.3.3 Solar Wind	12
1.3.4 Magnetosphere	13

1.4	Magnetic Reconnection	15
1.5	Magnetic Islands	17
1.6	Harris Current Sheet	18
1.7	Turbulence	19
1.8	Spacecraft Observations	23
1.9	Objective and Outline of This Thesis	25
1.10	Chapter Wise Summary of the Thesis	25-28

2. Nonlinear dynamics of kinetic Alfvén and whistler waves in the solar wind

2.1	Introduction	29
2.2	Kinetic Alfvén wave dynamics	31
2.3	Quasi-transverse whistler wave dynamics	35
2.4	Numerical Simulation	41
2.5	Simplified Model	42
2.6	Discussion and Conclusion	46

3. Trapping and amplification of quasi-longitudinal whistler wave in kinetic Alfvén wave localized structures

3.1	Introduction	51
3.2	Quasi-longitudinal whistler wave Dynamics	53
3.3	Numerical Simulation	55
3.4	Simplified Model	56

3.5 Discussion and Conclusion	59
-------------------------------	----

4. Effect of magnetic islands on the localization of kinetic Alfvén wave

4.1 Introduction	61
4.2 Kinetic Alfvén wave dynamics	64
4.3 Numerical Simulation	65
4.4 Simplified Model	67
4.5 Discussion and Conclusion	69

5. Nonlinear effects associated with kinetic Alfvén wave in reconnection region and turbulence generation

5.1 Introduction	73
5.2-I kinetic Alfvén wave dynamics	75
5.3-I Numerical Simulation and results	76
5.4-I Simplified Model	78
5.5-I Discussion	86
5.2-II Kinetic Alfvén wave dynamics	87
5.3-II Numerical Simulation and results	91
5.4-II Simplified Model	92
5.5-II Discussion	97
5.6 Summary of the Chapter	99

6. The study of turbulent magnetic field reconnection in the presence of guide field: Effect of electron physics

6.1	Introduction	99
6.2	Basic Formulations	100
6.3	Numerical Simulation	102

7. Summary of the present work and scope of the future work

107

References

110

List of Research Publications

118

BIO-DATA of the Author

119

LIST OF FIGURES

Number	Description	Page
Figure (1.1)	Image for the solar wind.	12
Figure (1.2)	Illustration of a steady state solar wind-magnetosphere system of Earth's environment in the meridian plane.	14
Figure (1.3)	Sweet-Parker reconnection.	15
Figure (1.4)	Schematic illustration of energy spectrum of fluid turbulence.	20
Figure (2.1)	Transient evolution of (i) intensity and (ii) respective contour plot of 3D KAW at (a) $t=1$, (b) $t=6$ and (c) $t=12$ at fixed z .	47
Figure (2.2)	Transient evolution of (i) intensity and (ii) respective contour plot of whistler wave at (a) $t=1$, (b) $t=6$ and (c) $t=12$ at fixed z .	48
Figure (2.3)	Power spectrum of 3D KAW at $t=9$.	49
Figure (2.4)	Power spectrum of whistler wave at $t=12$.	49
Figure (2.5)	Localization of i (a) 3D KAW and i (b) whistler wave by semi-analytical model in $r-z$ and $x-z$ plane respectively.	50
Figure (3.1)	The field intensity of 3D KAW obtained by numerical simulation at (a) at $t = 0$ (b) at $t=3$ (c) at $t=5$.	59
Figure (3.2)	The intensity of whistler wave, propagating at an angle $\theta=90^\circ$ with magnetic field, obtained by numerical simulation at (a) $t = 0$ (b) at $t = 3$ (c) at $t=12$.	60

- Figure (3.3)** (a)The localization of whistler wave by semi-analytical model in y-z plane ($x=0$) (b) the localization of whistler wave by semi-analytical model in x-z plane ($y=0$). 60
- Figure (4.1)** The spatial variation of in (a) x-z plane and (b) y-z plane obtained by numerical simulation for three different values of b_0 : (i) $b_0=0.5$, (ii) $b_0=0.7$ and (iii) $b_0=0.8$. 70
- Figure (4.2)** Plot of current density in x-y plane at different values of z : (a) $z=2$ (b) $z=4$ (a) $z=10$ (c) $z=15$. 71
- Figure (4.3)** The distribution of vector potential of KAW in (a) x-z plane and (b)y-z plane obtained semi-analytically for two values of b_0 : (i) $b_0=0.5$, and (ii) $b_0=0.8$. 72
- Figure (5.1)** The localization of KAW in presence of density modification in the background density, obtained at (a) $z=0$ (b) $z=4$ (c) $z=30$. 81
- Figure (5.2)** The localization of KAW in presence of pre-existing fully developed chain of magnetic islands (only), obtained at (a) $z=0$ (b) $z=4$ (c) $z=30$. 81
- Figure (5.3)** The localization of KAW in presence of density modification in the background density and pre-existing fully developed chain of magnetic islands(both), obtained at (a) $z=0$ (b) $z=4$ (c) $z=30$. 83
- Figure (5.4)** Plot of (i) magnetic flux and (ii) current density in the presence of density modification in the background density and pre-existing fully developed chain of magnetic islands, in x-y plane at different values of z : (a) $z=0$ (b) $z=4$ and (c) $z=30$. 83

Figure (5.5)	The saturated averaged wave number power spectrum between $z=28$ to $z=33$.	84
Figure (5.6)	Plot of scale size verses critical magnetic field strength using simplified model.	84
Figure (5.7)	The localization of KAW due to presence of (i) pre-existing fully developed chain of magnetic islands (only) and (ii) density modification in the background density as well as pre-existing fully developed chain of magnetic islands (both) obtained semi-analytically.	85
Figure (5.8)	Plot of (i) magnetic flux and (ii) current density in presence of density perturbation and Harris sheet (both), in x-y plane at different values of t: (a)t=1 (b)t=9 and (c) t=19.	95
Figure (5.9)	The saturated averaged wave number power spectrum between $t=10$ to $t=28$.	96
Figure(5.10)	Scale sizes verses critical magnetic field strength using simplified model.	96
Figure(5.11)	The localization of KAW due to presence of density modification in the background density as well as Harris sheet (both).	97
Figure (6.1)	(a-d) are the contour plot of vector potential (A_z) in x-y plane due to sole presence of Harris equilibrium field (absence of axial field) at different times viz. (a) $t=1$ (b) $t=5$ (c) $t=15$ and (d) $t=45$.	104
Figure (6.2)	a-d) are the contour plot of vector potential (A_z) in x-y plane due to the simultaneous presence of axial field as	

well as Harris field at different times viz. (a) $t=1$ (b) $t=4$
(c) $t=9$ and (d) $t=15$.

105

Figure (6.3) Turbulent spectrum resulting due to the simultaneous
present of axial field and Harris equilibrium field.

106